

Determination of Momentum Transfer and Inelastic Collision Cross Sections for Electrons in Nitrogen Using Transport Coefficients*

A. G. ENGELHARDT, A. V. PHELPS, AND C. G. RISK†

Westinghouse Research Laboratories, Pittsburgh, Pennsylvania

(Received 27 April 1964)

Momentum transfer and inelastic collision cross sections for electrons in N_2 have been obtained from electron transport coefficients for values of the electron energy between about 0.003 and 30 eV. The recently proposed polarization correction to the rotational excitation cross sections of Gerjuoy and Stein leads to less satisfactory agreement between theory and experiment than do the unmodified cross sections. The cross sections for vibrational excitation are consistent with those of Schulz provided the total cross section is normalized to 5.5×10^{-16} cm² at 2.2 eV. Furthermore, a tail extending down to the threshold of 0.29 eV is postulated for the $v=1$ vibrational level. Electronic excitation is approximated by a set of six effective cross sections which, for the most part, are consistent with previous results. The ionization cross section of Tate and Smith was used. The mean energy of electrons in N_2 subjected to high-frequency ac electric fields is found to be a single-valued function of the electric field E divided by the ac radian frequency ω , although there are regions of E/ω where the mean energy increases extremely rapidly with E/ω .

I. INTRODUCTION

THIS paper presents the results of an investigation to determine momentum transfer and inelastic collision cross sections for electrons in N_2 using transport coefficients. Previously, studies¹⁻³ have been made of H_2 , D_2 , and Ar, and in addition, Frost and Phelps¹ (hereafter called I) have reported some initial calculations for the rotational region of N_2 . In this work we shall discuss the extension of the studies for N_2 in I to higher energies and present a somewhat more detailed analysis of the rotational region.

As in the analysis of H_2 by Engelhardt and Phelps² (hereafter called II), we consider three separate regions of the characteristic energy⁴ ϵ_K given by

$$\epsilon_K = eD/\mu, \quad (1)$$

where e is the electronic charge, D is the diffusion coefficient, and μ is the mobility. The first region, designated as *A*, starts at thermal values of ϵ_K ; here elastic scattering and rotational excitation are the significant collision processes. Since the nitrogen is at 77°K, region *A* is delineated by ϵ_K varying from approximately 0.007 to 0.08 eV. Our studies of region *A* have investigated in detail the effect of the polarization correction suggested by Dalgarno and Moffett⁵ and independently by Mjolsness and Sampson.⁶ In region *B* where ϵ_K varies from 0.08 to 1.3 eV, elastic scattering, and rotational and vibrational excitation are the domi-

nant collision processes. In the case of vibrational excitation, we have relied heavily on the measurements by Schulz⁷⁻⁹ for the determination of cross sections. For $\epsilon_K > 1.3$ eV, i.e., region *C* where electronic excitation is significant, we have constructed a set of equivalent excitation cross sections whose thresholds are based on Schulz' measurements.⁷ The data of Tate and Smith¹⁰ served as the basis for the ionization cross section used. Finally, over the entire region of interest,

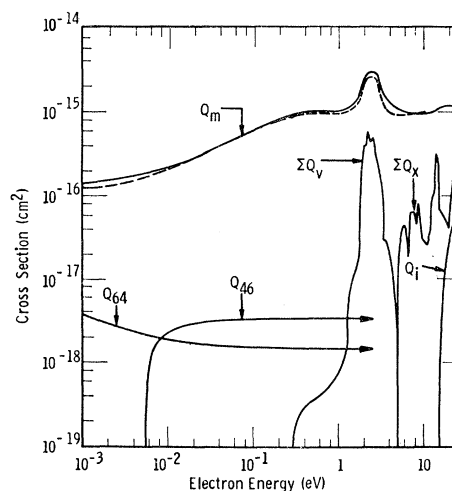


FIG. 1. Momentum transfer Q_m and inelastic collision cross sections for electrons in N_2 . The dashed Q_m curve indicates the results reported previously by Frost and Phelps. To avoid confusion we show only the curves for rotational excitation at 77°K from $J=4$ to $J=6$ and de-excitation from $J=6$ to $J=4$ calculated for a quadrupole moment \mathcal{Q} of 1.04 in atomic units using the theory of Gerjuoy and Stein. The curve labeled ΣQ_v represents the total of all the vibrational cross sections from $v=1$ to 8, as the curve labeled ΣQ_x represents the total of all six effective excitation cross sections with thresholds between 5.0 and 14.0 eV. The ionization cross section Q_i represents the experimental results of Tate and Smith.

* This research was sponsored in part by the U. S. Air Force Weapons Laboratory.

† Present address: Massachusetts Institute of Technology, Cambridge, Massachusetts.

¹ L. S. Frost and A. V. Phelps, Phys. Rev. **127**, 1621 (1962).

² A. G. Engelhardt and A. V. Phelps, Phys. Rev. **131**, 2115 (1963).

³ A. G. Engelhardt and A. V. Phelps, Phys. Rev. **133**, A375 (1964).

⁴ Equation II. (1) refers to Eq. (1) of II. Here we use precisely the same notation as in II.

⁵ A. Dalgarno and R. J. Moffett, Indian Academy of Sciences Symposium on Collision Processes, 1962 (unpublished).

⁶ R. C. Mjolsness and D. H. Sampson, Bull. Am. Phys. Soc. **9**, 187 (1964).

⁷ G. J. Schulz, Phys. Rev. **116**, 1141 (1959).

⁸ G. J. Schulz, Phys. Rev. **125**, 229 (1962).

⁹ G. J. Schulz, Phys. Rev. **135**, A988 (1964).

¹⁰ J. T. Tate and P. T. Smith, Phys. Rev. **39**, 270 (1932).

i.e., electron energy $\epsilon \leq 30$ eV, we have determined a momentum transfer cross section which is consistent with most of the experimental data.

As in II, we have calculated distribution functions and transport coefficients for electrons subjected to high-frequency electric fields. In particular, we have been able to investigate the somewhat unusual behavior of the high-energy portion of the distribution function and of the average electron energy at high frequencies in N_2 .

Our technique is virtually unchanged from that described in I and II, and consequently, a detailed description will be omitted. We solve numerically the time- and space-independent Boltzmann transport equation for the distribution function of electron energies in a neutral gas. Then, by suitable averages of appropriate cross sections over this distribution function, we are able to determine the various transport coefficients of interest. We then compare calculated and experimental values of these transport coefficients and make the appropriate adjustments in the momentum transfer and inelastic collision cross sections until a satisfactory fit is obtained.

II. DETERMINATION OF CROSS SECTIONS

Region A: Elastic Scattering and Rotational Excitation [$(kT/e) < \epsilon_K < 0.08$ eV]

Shown in Fig. 1 are our best values for the momentum transfer cross section Q_m and sample curves for rotational excitation between states with rotational quantum numbers $J=4$ and $J=6$, and for rotational de-excitation from $J=6$ to $J=4$. The dashed Q_m curve indicates the results reported previously in I. The rotational curves shown were found using the theory of Gerjuoy and Stein.¹¹ As indicated below the application of the polarization correction proposed by Dalgarno and Moffett⁵ and Mjolsness and Sampson⁶ does not allow us to improve the agreement with experiment. For clarity, we have plotted only Q_{46} and Q_{64} as calculated using a quadrupole moment \mathcal{Q} of 1.04 in units of ea_0^2 and no polarization correction.

In order to solve the Boltzmann transport equation accurately in region A, it is necessary to include inelastic collisions of the second kind, i.e., superelastic collisions. As discussed in I, the threshold energy for the lowest lying rotational level of N_2 is only 1.5×10^{-3} eV, a value which is significantly less than the 77°K thermal value of $\epsilon_K = 0.00663$ eV, so that a large number of rotational excitation and de-excitation cross sections must be considered. For ϵ_K varying from kT/e to approximately $3kT/e$ when $T = 77^\circ\text{K}$, the required number of rotational levels excited is manageable and we have used the exact expressions as given by Eqs. II. (18)–(24). For $\epsilon_K > 3kT/e$, it was necessary to replace the exact set of cross sections by an approximate

¹¹ E. Gerjuoy and S. Stein, Phys. Rev. **97**, 1671 (1955); **98**, 1848 (1955).

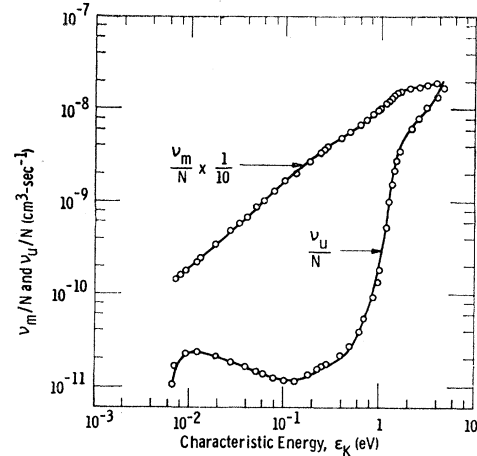


Fig. 2. Effective momentum transfer ν_m and energy exchange ν_u collision frequencies for electrons in N_2 at 77°K normalized to the neutral particle density N . The points represent our theoretical calculations using no polarization correction and $\mathcal{Q} = 1.04 ea_0^2$, and the smooth curves represent an average of the best available experimental data.

set¹ whose thresholds had been increased by a factor of 2 and whose magnitudes were appropriately decreased. The correctness of this approximation was tested in the region around $\epsilon_K = 3kT/e$, where it was possible to use both methods; it was found that the results agreed to within a few percent. For $\epsilon_K \geq 7kT/e$ (i.e., 0.046 eV) the continuous approximation for the rotational cross sections derived in I yields results accurate to within a few percent.

Shown in Fig. 2 are plots displaying our calculated momentum transfer and energy exchange collision frequencies, i.e., ν_m and ν_u , respectively, shown as points. Averages of the best available experimental data are shown as smooth curves. In the case of the ν_m/N curve, the satisfactory agreement vindicates our final choice of the Q_m curve. As for the ν_u/N plot, the calculated points are for rotational cross sections computed using no polarization correction and $\mathcal{Q} = 1.04 ea_0^2$. We consider the agreement to be reasonably good since the maximum discrepancy does not exceed 5% for $\epsilon_K > 0.01$ eV. As pointed out in I, the ν_m/N versus ϵ_K curve is very insensitive to the assumed values of the inelastic collision cross sections.

The effect of the theoretical polarization correction and of the sign and magnitude of the quadrupole moment is explored in greater detail in Fig. 3, where we show the experimental results as a smooth curve and the various calculations as points. The triangles are for a polarization correction¹² using a positive quadrupole moment of $\mathcal{Q} = +0.974 ea_0^2$ [see Eqs. II. (23) and (24)]. This curve is fitted to experiment at $\epsilon_K \approx 0.012$ eV since the theory is most accurate near threshold

¹² The parallel and perpendicular polarizabilities used for N_2 are 16.1 and 9.8 in a.u. See J. O. Hirschfelder, C. F. Curtis, and R. B. Bird, *Molecular Theory of Gases and Liquids* (John Wiley & Sons, Inc., New York, 1954).

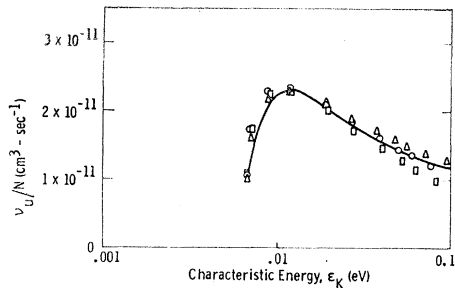


FIG. 3. Energy exchange collision frequency ν_u for electrons in N_2 at 77°K normalized to N . We show primarily the region where elastic scattering and rotational excitation are important. The smooth curve represents an average of the best available experimental data. The circles represent our calculated results for no polarization correction and $\mathcal{Q}=1.04 ea_0^2$; the triangles represent calculations for a polarization correction and $\mathcal{Q}=+0.974 ea_0^2$; and the squares represent those for a polarization correction and $\mathcal{Q}=-1.10 ea_0^2$.

and since experiments should be reasonably accurate in this region. An acceptable fit to the ν_u/N data near $\epsilon_K=0.012$ eV for a polarization correction using a negative quadrupole moment of $\mathcal{Q}=-1.10 ea_0^2$ is shown by the squares. The circles indicate that a value of $\mathcal{Q}=1.04 ea_0^2$ produces good results when no polarization correction is used. A comparison of the three curves of Fig. 3 yields the conclusion that the use of a polarization correction, whether positive or negative, does not improve the agreement with experiment. A similar conclusion would have been reached had we used a least-squares fit for the same three cases for $\epsilon_K>0.01$ eV.

This conclusion supersedes that stated previously,¹³ but is consistent with recent¹⁴ theoretical investigations which indicate that the effect of the polarization correction using a negative¹⁵ quadrupole moment is at least partially cancelled by other corrections. The magnitude of the quadrupole moment determined by our analysis appears to be in good agreement with most recent determinations as summarized by Poll¹⁶ and Ketelaar and Rettschnick,¹⁷ although the effect of averaging^{1,2} over the internuclear separation does not appear to have been taken into account.

A direct comparison of the results of our calculations with experiment is furnished by Fig. 4 in terms of drift velocity and characteristic energy plots. Here the calculations for $\mathcal{Q}=1.04 ea_0^2$ and $T=77^\circ\text{K}$ are shown as smooth curves, and the various experimental re-

sults¹⁸⁻²⁸ are shown as points. The agreement (in region A) with the ϵ_K data of Warren and Parker²⁵ and the w data of Lowke¹⁹ is excellent. A typical electron energy distribution function which is characteristic of this range of ϵ_K is shown in Fig. 12. This energy distribution is intermediate between Maxwellian and Druyvesteyn.¹

Region B: Elastic Scattering, Rotational Excitation and Vibrational Excitation [$0.08 \leq \epsilon_K \leq 1.4$ eV]

Above $\epsilon_K \approx 0.1$ eV, a significant number of electrons possess energy in excess of the excitation energy²⁹ (0.29 eV) of the $v=1$ vibrational level, and vibrational excitation must be taken into account. For energies above 1.7 eV, the relative magnitudes and shapes of the eight vibrational cross sections, i.e., from $v=1$ to $v=8$, are the same as those given by Schulz.^{8,9} We show the sum of these as $\sum Q_v$ in Fig. 1. Of particular significance is the tail of the $v=1$ cross section. We have found it necessary to add this tail to the $v=1$ cross section in order to obtain agreement with the experimental data.

The tail we have added is shown in greater detail in Fig. 5 as the solid line labeled Q_{01} . The dashed line indicates the result calculated by Chen.³⁰ Below 1.2 eV we have chosen his values since they give a good fit. Above 1.2 eV we have found it necessary to use a cross section significantly larger than his. This discrepancy cannot be accounted for by the uncertainty in the shape of the rotational excitation cross sections. The points shown in Fig. 5 represent the lowest energy data of Schulz.⁹ Because of the low sensitivity of his apparatus, Schulz could not study this threshold region accurately, and, therefore, the disagreement is not considered to be significant. Also shown is the cross section Q_{10} for vibrational de-excitation calculated using detailed balancing.³¹ The excellent results using this tail with a quadrupole moment of $1.04 ea_0^2$ are shown in

¹³J. L. Pack and A. V. Phelps, Phys. Rev. **121**, 798 (1961).

¹⁹J. J. Lowke, Australian J. Phys. **16**, 115 (1963). Because the results of Bortner *et al.* [T. E. Bortner, G. S. Hurst, and W. G. Stone, Rev. Sci. Instr. **28**, 103 (1957)] and J. C. Bowe [Phys. Rev. **117**, 1411 (1960)] are consistently lower than those of Lowke, we have not plotted the former in Fig. 4.

²⁰N. E. Bradbury and R. A. Nielsen, Phys. Rev. **49**, 388 (1936).

²¹D. Errett, Ph.D. thesis, Purdue University, 1951 (unpublished).

²²K. H. Wagner and H. Raether, Z. Physik **170**, 540 (1962).

²³W. Riemann, Z. Physik **122**, 216 (1944).

²⁴L. Frommhold, Z. Physik **160**, 554 (1960).

²⁵R. W. Warren and J. H. Parker, Phys. Rev. **128**, 2661 (1962).

²⁶J. S. Townsend and V. A. Bailey, Phil. Mag. **42**, 873 (1921).

²⁷R. W. Crompton and M. T. Elford, *Proceedings of the Sixth International Conference on Ionization Phenomena in Gases* (Paris, 1963).

²⁸L. W. Cochran and D. W. Forester, Phys. Rev. **126**, 1785 (1962). Only data for $\epsilon_K>0.2$ eV is shown since the experiments were carried out at 298°K rather than 77°K.

²⁹G. Herzberg, *Spectra of Diatomic Molecules* (D. Van Nostrand Company, Inc., Princeton, New Jersey, 1950).

³⁰J. C. Y. Chen (private communication, 1963).

³¹A. C. G. Mitchell and M. W. Zemansky, *Resonance Radiation and Excited Atoms* (Cambridge University Press, New York, 1934).

¹³A. G. Engelhardt, A. V. Phelps, and C. G. Risk, Bull. Am. Phys. Soc. **9**, 187 (1964).

¹⁴D. H. Sampson and R. C. Mjolsness (private communication, 1964).

¹⁵C. W. Scherr, J. Chem. Phys. **23**, 569 (1955). The negative sign has been recently confirmed theoretically by P. Cade, K. D. Sales, and A. C. Wahl (private communication); Bull. Am. Phys. Soc. **9**, 102 (1964).

¹⁶J. D. Poll, Phys. Letters **7**, 32 (1963).

¹⁷J. A. Ketelaar and R. P. H. Rettschnick, Mol. Phys. **7**, 191 (1963-64).

FIG. 4. Drift velocity w and characteristic energy ϵ_K for electrons in N_2 at 77°K. The points represent the various experimental results and the smooth curves our computations for no polarization correction and $\varrho = 1.04 ea_0^2$.

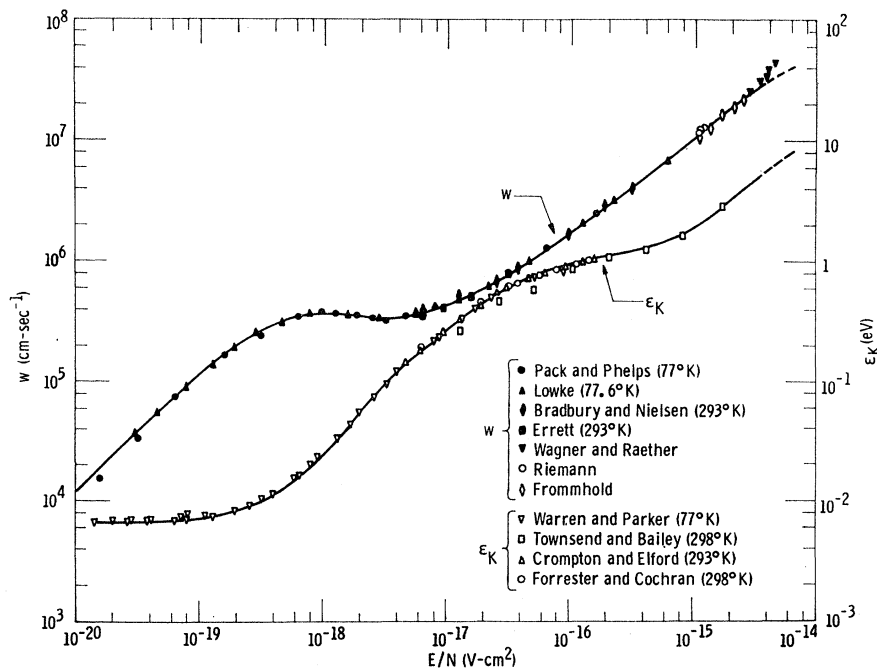


Fig. 2. The parameter ν_u/N is quite sensitive to variations in the tail for $0.1 \leq \epsilon_K \leq 0.5$ eV. If the tail is deleted our calculated points fall well below the experimental line. Increasing the magnitude of higher energy portions of the vibrational cross sections has little effect on ν_u/N for $\epsilon_K \leq 0.5$ eV.

For $0.5 \leq \epsilon_K \leq 1.3$ eV, the higher energy portion of the $v=1$ cross section, and the $v=2$ to 8 processes are the significant vibrational cross sections. In order to obtain the acceptably good agreement with the experimental ν_u/N data shown in Fig. 2, it was necessary to normalize $\sum Q_v$ to 5.5×10^{-16} cm² at 2.2 eV. This is to be compared with a value of 3.8×10^{-16} cm² obtained by Haas³² and a value ranging from 3.3 to 5.8×10^{-16} cm², depending on scattering angle, given by Schulz.⁹

Our final Q_m curve applicable to this region of ϵ_K is confirmed by the good agreement for the ν_m/N plot. In terms of a comparison of calculated and experimental values of w and ϵ_K , we see from Fig. 4 that the agreement is quite good with all but one set of experimental data. The disagreement with the Townsend and Bailey²⁶ ϵ_K data is reminiscent of previous discrepancies^{2,3} in H_2 and in Ar.

Region C: Elastic Scattering, Rotational, Vibrational, and Electronic Excitation, and Ionization [$\epsilon_K > 1.3$ eV]

For $\epsilon_K > 1.3$ eV the complexity of the analysis is increased by the growing importance of excitation processes whose thresholds and energy losses are equal

³² R. Haas, Z. Physik 148, 177 (1957).

to or are in excess of 5.0 eV. To simplify the analysis as much as possible, we have chosen to ascribe energy loss in this region to a small number of inelastic processes; namely, seven excitation and ionization cross sections as shown in Fig. 6. We rely heavily on the measurements by Schulz⁷ who used the trapped elec-

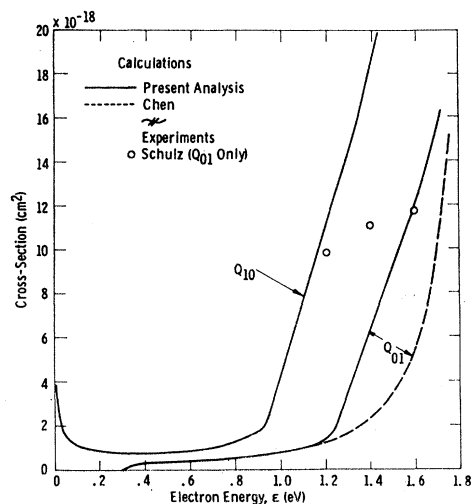


FIG. 5. Low-energy portion or "tail" of the $v=1$ vibrational cross section in the region where the electron energy $\epsilon \leq 1.7$ eV. The derived cross section Q_{01} for vibrational excitation, and the cross section Q_{10} for vibrational de-excitation calculated using detailed balancing are shown as solid curves. The curve derived by Chen for Q_{10} is shown as a dashed line. Below 1.2 eV his results and ours are identical. The points represent the experimental results of Schulz for Q_{01} when normalized to our value for the sum of the vibrational excitation cross sections of 5.5×10^{-16} cm² at 2.2 eV.

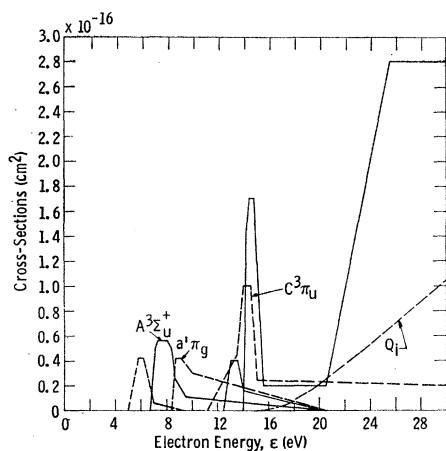


FIG. 6. Effective excitation cross sections with thresholds between 5.0 and 14.0 eV and the ionization cross section Q_i . The three excitation processes which have been clearly identified are the $A^3\Sigma_u^+$, the $a^1\pi_g$, and the $C^3\pi_u$. These three levels have thresholds at 6.7, 8.4, and 11.2 eV, respectively. The other three whose exact nature is as yet undetermined have thresholds at 5.0, 12.5, and 14.0 eV. The solid and dashed curves have been used solely for the purpose of clarity in presentation.

tron method to deduce the behavior of excitation cross sections near threshold. Schulz observed three excitation processes which he was able to identify as the $A^3\Sigma_u^+$ state with a threshold at 6.7 eV, the $a^1\pi_g$ state with a threshold at 8.4 eV and the $C^3\pi_u$ state with a threshold at 11.2 eV. In addition to the three processes just discussed Schulz' data also suggest the presence of three unidentified processes with thresholds in the vicinity of 5 eV (presumably vibrational excitation), 12.5 and 14 eV. We have found it desirable to include cross sections for these six processes and have used the threshold energy as suggested by the peaks in Schulz' data. It should be noted that with N_2 significant errors result from the use of effective excitation cross sections which are too widely spaced. This is because the large vibrational excitation cross section beginning at 1.7 eV acts as a barrier to the gain of energy by electrons which re-enter the distribution at energies below 1.7 eV after an inelastic collision. Electrons re-entering above 2.9 eV do not experience this barrier. Figure 6 displays the effective vibrational and electronic excitation cross sections we have used to obtain the best fit with experimental data.

As in I and II, it must be emphasized that our derived cross sections are a reasonably realistic set but that they are not unique. The "C" state excitation cross section which we have used is in reasonable agreement with recent results of Schulz,^{7,33} of Stewart and Gabathuler,³⁴ and of Legler,³⁵ but peaks at a signifi-

cantly lower energy than that obtained by Kishko.³⁶ However, the additional large cross sections at energies near 14.5 eV, which were found in this analysis to be necessary in order to fit the δ/N data discussed below, have not been observed to date in any direct experimental measurement of cross sections. Similarly, direct experimental evidence has not been obtained for the rapidly rising cross section at energies above 20 eV. In our analysis this cross section was assigned to the 14-eV level for convenience. The energy loss associated with this cross section may well correspond to some process in which most of the excitation energy is dissipated in radiation or dissociation rather than ionization. Evidence for this type of process has been obtained by Przybylski,³⁷ although his analysis yields an excitation coefficient which is too small to account for the energy losses. If this excitation process does have an energy loss near 20 eV, then the total cross section required will be significantly smaller than that shown in Fig. 1. Note that except for the C state, the cross sections given in Fig. 6 may not give accurate excitation rates for the individual states when E/N is high enough so that cross sections significantly above threshold are important.

For the ionization cross section Q_i we have used the results of Tate and Smith¹⁰ as shown in Figs. 1 and 6. Sample calculations were performed using three ionization cross sections with different thresholds as given by Fox³⁸ rather than the single one beginning at 15.6 eV. As long as the sum of the three ionization cross sections was normalized to the same value as the single one, no significant differences were found to exist in the transport coefficients.

In region C in addition to the ν_u/N and ν_m/N data,

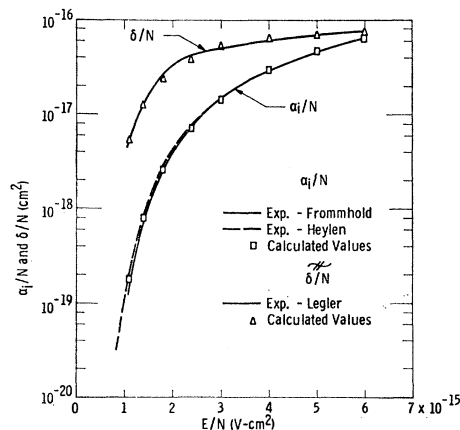


FIG. 7. Ionization coefficient α_i and photon excitation coefficient δ for electrons in N_2 normalized to N . δ is associated with the $C^3\pi_u$ state. Our calculations are shown as points and the various experimental results as smooth curves.

³³ G. J. Schulz (private communication, 1963).

³⁴ D. T. Stewart and E. Gabathuler, Proc. Phys. Soc. (London) **72**, 287 (1958). We have assumed that the apparent threshold found in these measurements can be shifted to 11.2 eV.

³⁵ W. Legler, Z. Physik **173**, 169 (1963).

³⁶ S. M. Kishko, Opt. i Spektroskopiya **8**, 160 (1960) [English transl.: Opt. Spectry. (USSR) **8**, 84 (1960)].

³⁷ A. Przybylski, Z. Physik **168**, 504 (1962).

³⁸ R. E. Fox, J. Chem. Phys. **35**, 1379 (1961).

we have recourse to two other experimentally determined transport coefficients—the photon excitation coefficient for the C state δ and the ionization coefficient α_i . Both of these coefficients were calculated using Eqs. II. (10) and (10a). Our procedure in determining excitation cross sections for this region has been first to base our initial estimates primarily on the results of Schulz.⁷ A comparison (with experimental results) of calculated values of ν_u , δ , and α_i resulting from the cross sections so obtained led to subsequent revision until acceptable agreement was obtained for all three coefficients.

Figure 7 shows plots of δ and α_i both normalized to the neutral particle density N . The experimental results of Frommhold,²⁴ Heylen,³⁹ and Legler³⁵ are shown as smooth curves and our calculated results as points. In the case of α_i/N the agreement is essentially perfect, but it should be noted that this agreement was obtained for the higher values of E/N by postulating the somewhat unusual shape for the 14-eV process above 20 eV. We were unable to reduce the residual errors of the order of 10% which remain in the δ/N plot in the region $1.5 \times 10^{-15} \leq E/N \leq 2.5 \times 10^{-15}$ V-cm². The ν_u/N results shown in Fig. 2 for region C are considered acceptable.

An additional point to be emphasized in connection with the δ/N and α_i/N plots is that above $E/N = 3.5 \times 10^{-15}$ V-cm² over 10% of the total energy input from the field to the electrons is being consumed in the ionization process. Since we have neglected the presence of the extra electron produced in the ionization process, the accuracy of the results above this value of E/N is open to question, and they are shown as dashed lines in Fig. 4.

The momentum transfer cross section derived for region C and shown in Fig. 1 is about 20% smaller than that given by Frost and Phelps for energies above about 2 eV. Our $Q_m(\epsilon)$ curve is therefore about 20% lower than the total cross section given by Brode,⁴⁰ but is found to be consistent with mobility and ϵ_K data by Heylen.⁴¹ The difference between the total cross section and our Q_m curve is typical of the behavior found in the rare gases.⁴²

The behavior of the distribution function $f(\epsilon)$ in regions B and C is illustrated⁴³ by Fig. 8 where we show $f(\epsilon)$ plotted against ϵ in eV for three values of ϵ_K . At the lowest value of ϵ_K , i.e., 1.0 eV, vibrational excitation is by far the dominant process. The precipitous decrease in $f(\epsilon)$ near 2.0 eV indicates there

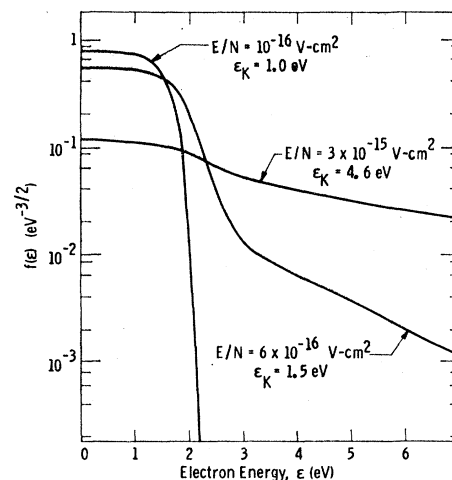


FIG. 8. Energy distribution functions $f(\epsilon)$ for electrons in N_2 for three values of E/N and corresponding values of ϵ_K . $f(\epsilon)$ is defined such that $\int_0^\infty \epsilon^{1/2} f(\epsilon) d\epsilon = 1$.

are few electrons able to pass the peak of the total vibrational cross section which, therefore, acts almost as an impenetrable barrier. In addition, at low energies the behavior of $f(\epsilon)$ is highly non-Maxwellian as is the case for the other two cases shown, viz., $\epsilon_K = 1.5$ and 4.6 eV. For $\epsilon_K = 1.5$ eV a substantial number of electrons have energies in excess of 2.2 eV and a high-energy tail is clearly in evidence. In the case of $\epsilon_K = 4.6$ eV, the highest value shown, the tail is quite pronounced and extends well into the region of the high-energy electronic excitation processes. Similar plots of $f(\epsilon)$ for air have been reported by Carleton and Megill.⁴⁴

III. ADDITIONAL CALCULATIONS

In this section we use the results of the previous section to examine the fraction of the input energy dissipated in each of the collision processes. We also use these results to predict the variation of the ratio of the "magnetic drift velocity"^{1,8} to the time-of-flight drift velocity with E/N , and of the mean electron energy with the strength of a very-high-frequency electric field.

A. Fractional Energy Loss

We examine the power input from the electrons to the various elastic and inelastic processes as a means of delineating the different regions of dominance and scrutinizing to some extent the sensitivity of the analysis. Figure 9 shows plots of the fractional power input to elastic and inelastic collisions versus E/N ; an ϵ_K scale has been added for convenience. Because the continuous approximation to rotation has been used for $E/N > 3.0 \times 10^{-18}$ V-cm² we have not separated the power input to elastic collisions from that to rotational excitation. The dashed lines indicate the region

³⁹ A. E. D. Heylen, *Nature* **183**, 1545 (1959).

⁴⁰ R. B. Brode, *Rev. Mod. Phys.* **5**, 257 (1933).

⁴¹ A. E. D. Heylen, *Proc. Phys. Soc. (London)* **79**, 284 (1962).

⁴² H. S. W. Massey and E. H. Burhop, *Electronic and Ionic Impact Phenomena* (Clarendon Press, Oxford, 1952), p. 15.

⁴³ The curves of Figs. 8, 11, and 12 were obtained from preliminary calculations performed using a polarization correction with a positive quadrupole moment of $+0.96 ea_0^2$. However, within the context of the discussion of these figures, the results shown do not differ significantly from those obtained using $\mathcal{Q} = 1.04 ea_0^2$ and no polarization correction.

⁴⁴ N. P. Carleton and L. R. Megill, *Phys. Rev.* **126**, 2089 (1962).

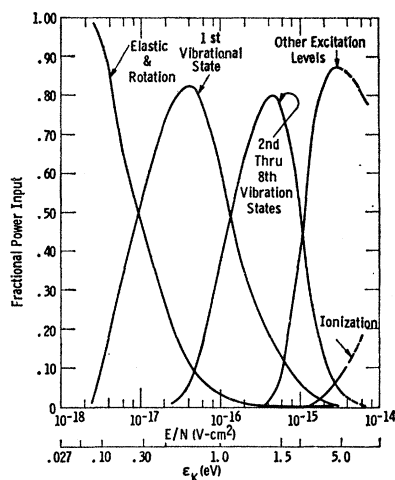


FIG. 9. Fractional power input to elastic and inelastic collisions for electrons in N_2 at $77^\circ K$ as a function of E/N . An ϵ_K scale has been inserted under the E/N scale for convenience. Because the continuous approximation to rotational excitation was used in the energy balance calculations we show combined the power input to elastic collisions and rotational excitation. As shown in I, the contribution of elastic collisions to the rate of energy loss is less than 10% of that for rotational excitation for $\epsilon_K < 0.1$ eV. In the interests of simplicity we have also summed the power input to all of the vibrational levels except the first and that to all other excitation levels with the exception of ionization. The fractional power inputs above $E/N = 3.5 \times 10^{-15}$ V-cm 2 are shown as dashed lines to indicate that in excess of 10% of the total power input is being consumed in ionization and that our results may be in error.

where the fractional power input to ionization is in excess of 10%, since as discussed previously the results in this region may be in error. A number of significant points emerge from a scrutiny of this figure. Up to $E/N = 9.0 \times 10^{-18}$ V-cm 2 most of the power is consumed in elastic collisions and rotational excitation. However, starting at $E/N = 3 \times 10^{-18}$ V-cm 2 , corresponding to $\epsilon_K = 0.10$, the power input to the first vibrational state (primarily the tail) rises rapidly until at $E/N = 4.0 \times 10^{-17}$ V-cm 2 over 80% of the power input is to this state. A similar situation exists for the 2nd through 8th vibrational states and the electronic excitation levels at higher E/N . As a result of this fairly good separation, we have been able to determine with quite acceptable accuracy the shape and magnitude of the tail of the $v=1$ state, the peak value of the total vibrational cross section and the effective electronic excitation cross sections.

B. Magnetic Deflection Data

Frost and Phelps¹ showed that the ratio of the "magnetic drift velocity" w_M to the time-of-flight drift velocity w is a moderately sensitive indication of the variation of the frequency of momentum transfer collisions with electron energy. The magnetic drift velocity is determined from measurements of the deflection of an electron swarm in a weak magnetic field.²⁶

With the increasing precision of measurements of electron transport coefficients,¹⁹ we expect that studies of this quantity will yield valuable information regarding the energy dependence of the momentum transfer collision frequency $\nu(\epsilon)$. Here $\nu(\epsilon) = (2e\epsilon/m)^{1/2} Q_m(\epsilon)$ is characteristic of monoenergetic electrons and is to be distinguished from ν_m/N shown in Fig. 2 which is a function of ϵ_K and is an effective value for all of the electrons. Now the "magnetic drift velocity" has been calculated by Townsend and Bailey²⁶ by the relation $w_M = (E/B) \tan \theta$, where θ is the angle through which a stream of electrons is deflected in a magnetic field B perpendicular to the electric field E . The value of w_M can be calculated from the electron energy distribution using the relation^{2,3}

$$w_M = (E/B)(\mu_l/\mu_T). \quad (2)$$

Since the time-of-flight drift velocity w is given by $w = \mu_l E$,

$$w_M/w = \mu_l/\mu_T \mu_l B. \quad (3)$$

In the limit of small magnetic fields this ratio⁴⁵ becomes

$$w_M/w = \mu_l/\mu^2 B, \quad (4)$$

and has previously¹ been called the "magnetic deflection coefficient." In the case of a momentum transfer collision frequency $\nu(\epsilon)$ which is independent of electron energy $w_M/w = 1$ for all E/N and B/N .

Calculated values of the low-magnetic field limit of w_M/w for N_2 at 77 and $300^\circ K$ are shown by the smooth curves of Fig. 10. The only experimental measurements of w_M are those of Townsend and Bailey²⁶ and when these are combined with the experimental time-of-flight data of Lowke¹⁹ one obtains the points shown in Fig. 10. The agreement between the calculated and experimental value is satisfactory over the limited range of E/N for which data are available. Two

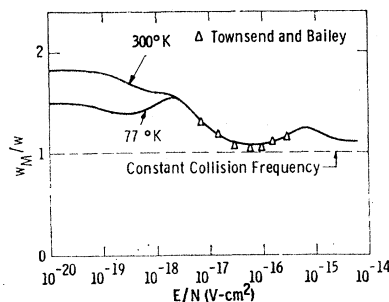


FIG. 10. Magnetic deflection coefficient w_M/w for electrons in N_2 at 77 and $300^\circ K$ in the low magnetic field limit. Our calculations are shown by the smooth curve and the experimental results of Townsend and Bailey by triangles. The dashed curve which represents $w_M/w = 1$ is the limiting value for a constant collision frequency, i.e., $Q_m \propto \epsilon^{-1/2}$.

⁴⁵ Two values of this ratio are plotted incorrectly in Fig. 4 of I. The correct value for the Maxwellian distribution and Q_m constant is 1.177 and that for a generalized Druyvesteyn distribution and $Q_m \propto \epsilon^{1/2}$ is 1.163.

regions of especial interest which have not been studied experimentally are the region near $E/N=6\times 10^{-16}$ V-cm² and the thermal region below $E/N=10^{-19}$ V-cm². The calculations for E/N near 6×10^{-16} V-cm² or $\epsilon_K=1.5$ eV show a peak in the value of w_M/w and indicate a greater energy dependence of the frequency of momentum transfer collisions for electrons in this energy range than for electrons with energies above or below this range. Such a behavior for $\nu(\epsilon)$ or $\epsilon^{1/2}Q_m(\epsilon)$ can be deduced from Fig. 1 for electrons with energies between 1.5 and 2 eV.

The curves of Fig. 10 for the thermal region, $E/N < 10^{-19}$ V-cm², show that w_M/w is calculated to be significantly larger at 300°K than at 77°K. We ascribe this to a more rapid variation⁴⁶ of the frequency of momentum transfer collisions for electrons with energies near 0.026 eV than for electrons near 0.0066 eV. This behavior can be deduced from the curve of $Q_m(\epsilon)$ in Fig. 1 which shows that $Q_m(\epsilon)$ approaches a finite value as $\epsilon \rightarrow 0$ such that $\nu(\epsilon)$ varies as $\epsilon^{1/2}$ rather than ϵ as is the case at higher electron energies. Also, the slight minimum in w_M/w near $E/N=3\times 10^{-19}$ V-cm² for 77°K is due to the fact that as E/N increases, there is a decrease in w_M/w resulting from a change in the energy distribution from Maxwellian to the generalized Druyesteyn⁴¹ for a given energy variation of the collision frequency (see I). Subsequently, w_M/w increases due to the increasing collision frequency.

These results show that measurements of the magnetic deflection coefficient and of the shape of cyclotron resonance peaks show a similar sensitivity⁴⁷ to energy variation of $\nu(\epsilon)$. This similarity is expected since, as was pointed out in I and II, the conductivity integrals used in the evaluation of ac experiments differ only by numerical coefficients from the mobility integrals applicable to dc measurements in the presence of crossed magnetic and electric fields. In particular, it is easily shown that if ω and $\omega_b=eB/m$ are numerically equal, then

$$\frac{w_M}{w} = \frac{\mu_{\perp}}{\mu_T \mu_{\parallel} B} = \frac{\sigma_i}{\sigma_r m \omega \sigma_r(\omega=0)}, \quad (5)$$

where σ_r and σ_i are the real and imaginary components of the ac conductivity parallel to the ac electric field when no magnetic field is present. In the presence of a magnetic field and in the usual experimental conditions,⁴⁸ the integral expressions for σ_r and σ_i are unchanged except for the substitution of $\omega-\omega_b$ for ω . Thus, for thermal electrons the right-hand side of Eq.

⁴⁶ For a Maxwellian distribution and $\nu(\epsilon)=a\epsilon^j$,

$$w_M/w = [\Gamma(\frac{5}{2}-j)\Gamma(\frac{3}{2})]/[\Gamma(\frac{5}{2}-j/2)]^2 \quad \text{when } j < \frac{5}{2}.$$

This expression is valid only for $\omega_b \ll \nu(\epsilon)$, where ω_b is the electron cyclotron frequency.

⁴⁷ L. R. Megill, F. C. Fehsenfeld, and L. K. Droppleman, Bull. Am. Phys. Soc. 9, 186 (1964).

⁴⁸ See, for example, F. C. Fehsenfeld, J. Chem. Phys. 39, 1653 (1963).

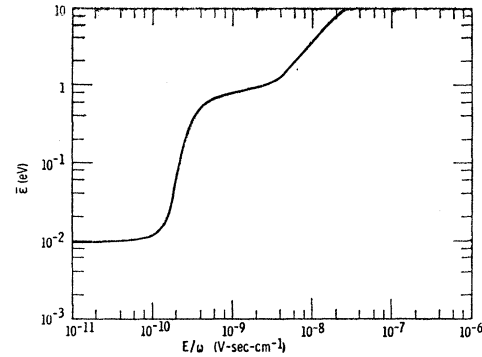


FIG. 11. Mean electron energy $\bar{\epsilon}$ of electrons in N₂ at 77°K as a function of E/ω at high frequencies. The calculations were performed for $\omega/N=6\times 10^{-7}$ cm³-sec⁻¹ when $E/\omega < 3.33\times 10^{-9}$ V-sec-cm⁻¹ and for $\omega/N=6\times 10^{-6}$ cm³-sec⁻¹ when $E/\omega > 3.33\times 10^{-9}$ V-sec-cm⁻¹.

(5) has the same value at cyclotron resonance ($\omega=\omega_b$) as w_M/w in Fig. 10 for $E/N \rightarrow 0$ and $B \rightarrow 0$.

C. AC Calculations

Most previous calculations of the behavior of electrons in N₂ subjected to high frequency, ac electric fields have made use of approximate forms for Q_m and $f(\epsilon)$. In particular, Altshuler⁴⁹ has derived expressions for the mean electron energy $\bar{\epsilon}$ based on the following three assumptions:

(i) The electrons lose energy to nitrogen molecules only by rotational excitation,

(ii) the effective electron collision frequency is a linear function of $\bar{\epsilon}$, and

(iii) the electron energy distribution function $f(\epsilon)$ is Maxwellian. Perhaps the most startling result of Altshuler's investigation is the prediction of a "hysteresis" effect in the curve of $\bar{\epsilon}$ as a function E/ω , where ω is the ac radian frequency. As may be inferred from the discussion in Sec. II the accuracy of all three assumptions is open to serious question. We have therefore made use of the cross sections determined in Sec. II to calculate the mean electron energy and the various measurable transport coefficients.

Plotted versus E/ω in Fig. 11 are our calculated⁴⁸ values of $\bar{\epsilon}$ found by computing the distribution function using the Boltzmann equation appropriate to the ac electric field² and the cross sections shown in Fig. 1. Perhaps the most important point to be noted is that $\bar{\epsilon}$ is a single-valued function of E/ω . The curve does not exhibit "hysteresis" or double-valued effects described by Altshuler although $\bar{\epsilon}$ does rise steeply in the regions where $10^{-10} \leq E/\omega \leq 4\times 10^{-10}$ V-sec-cm⁻¹ and $E/\omega \geq 2\times 10^{-9}$ V-sec-cm⁻¹. The explanation for the rather unusual behavior⁵⁰ of $\bar{\epsilon}$ with increasing E/ω is

⁴⁹ S. Altshuler, J. Geophys. Res. 68, 4707 (1963).

⁵⁰ A. V. Phelps, Natl. Bur. Std. Tech. Note No. 211, Vol. 5 (1964).

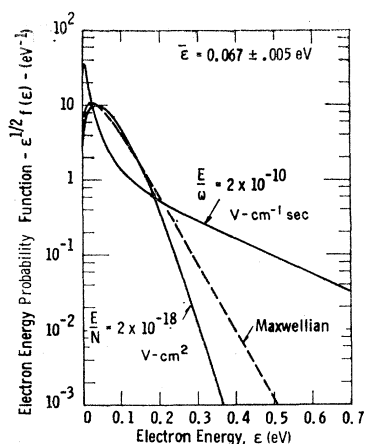


FIG. 12. ac and dc energy probability functions, $\epsilon^{1/2}f(\epsilon)$, for electrons in N_2 at 77°K when $\bar{\epsilon} = 0.067 \pm 0.005$ eV. $\epsilon^{1/2}f(\epsilon)d\epsilon$ is the probability of an electron having an energy between ϵ and $\epsilon + d\epsilon$. The dc case shown represents our calculated results when $E/N = 2.0 \times 10^{-18}$ V-cm 2 and $\omega = 0$. For comparison purposes we display the Maxwellian given by

$$\epsilon^{1/2}f(\epsilon) = [(27\epsilon/2\pi)(\bar{\epsilon})^{-3}]^{1/2} \exp(-3\epsilon/2\bar{\epsilon}).$$

found in Fig. 12 where we show⁴³ $\epsilon^{1/2}f(\epsilon)$ versus ϵ for a dc case $E/N = 1.2 \times 10^{-18}$ V-cm 2 , and for a very-high-frequency ac case, $E/\omega = 2 \times 10^{-10}$ V-sec-cm $^{-1}$ and $\omega/N = 6 \times 10^{-7}$ cm 3 -sec $^{-1}$. In addition, a Maxwellian energy probability function is also plotted. For all three cases, $\bar{\epsilon} = 0.067 \pm 0.005$ eV. Although the energy probability function in the dc case is intermediate between the Maxwellian and Druyvesteyn forms,¹ $\epsilon^{1/2}f(\epsilon)$ in the ac case peaks at very low energies and has a long tail at high energies. Since the energy loss processes are the same in both cases, the differences are due to the energy dependence of the energy gain term.^{2,49} At the highest $\bar{\epsilon}$ of Fig. 11, the electron energy probability functions for a given $\bar{\epsilon}$ are much more nearly independent of frequency because of the less rapid variation of the electron collision frequency with energy.

IV. CONCLUSIONS

By means of a numerical solution of the Boltzmann transport equation and subsequent comparison of calculated and experimental values of transport coefficients,⁵¹ we have derived a set of momentum transfer

⁵¹ A tabulation of the final values of the cross sections and calculated transport coefficients is available on request.

and inelastic collision cross sections for electrons in nitrogen. The gas temperature was taken to be 77°K corresponding to a thermal value of 0.00663 eV for the characteristic energy. From 0.003 to 30 eV a momentum transfer cross section has been found which is consistent with the experimental data. For rotational excitation we find that the theory of Gerjuoy and Stein gives a good fit to experiment using values of the quadrupole moment which are in agreement with most other recent determinations. The use of the polarization correction leads to less satisfactory agreement with experiment. Our cross sections for vibrational excitation are consistent with those of Schulz provided the total cross section is normalized to 5.5×10^{-16} cm 2 at 2.2 eV. In addition we have found it necessary to add to the $v=1$ vibrational cross section a tail extending down to the threshold of 0.29 eV. We have approximated electronic excitation by a set of six cross sections. The three of these which can be identified unambiguously are the $A^3\Sigma_u^+$, $a^1\pi_g$, and $C^3\pi_u$ states with thresholds at 6.7, 8.4, and 11.2 eV, respectively. The other three whose exact identity is unknown at present have thresholds at 5.0, 12.5, and 14.0 eV. The cross sections we have found for all six of these processes are consistent with Schulz' data. It was determined that a single-energy-loss ionization cross section beginning at 15.6 eV gives almost the same results as three ionization cross sections with different thresholds, provided that the sum of the three ionization cross sections is normalized to the same value as the single one. Finally, using the derived elastic and inelastic cross sections we conclude that the mean electron energy, $\bar{\epsilon}$, is a single-valued function of the electric field E divided by the ac radian frequency ω . However, there is a region of E/ω where $\bar{\epsilon}$ does increase very rapidly with increasing E/ω —so much in fact that if the distribution function is erroneously assumed to be Maxwellian and energy losses due to vibrational excitation are neglected, then $\bar{\epsilon}$ becomes a multivalued function of E/ω .

ACKNOWLEDGMENTS

The authors wish to express their thanks to L. S. Frost and G. J. Schulz for numerous helpful discussions. We are also indebted to G. J. Schulz for data furnished prior to publication.